

Tunneling Transverse to a Magnetic Field and Its Occurrence in Correlated 2D Electron Systems

T. Barabash-Sharpee,¹ M. I. Dykman,¹ and P. M. Platzman²

¹*Department of Physics and Astronomy, Michigan State University, East Lansing, Michigan 48824*

²*Bell Laboratories, Lucent Technologies, Murray Hill, New Jersey 07974*

(Received 21 April 1999)

We investigate tunneling decay in a magnetic field. Because of broken time-reversal symmetry, the standard WKB technique does not apply. The decay rate and the outgoing wave packet are found from the analysis of the set of the particle Hamiltonian trajectories and its singularities in complex space. The results are applied to tunneling from a strongly correlated 2D electron system in a magnetic field parallel to the layer. We show in a simple model that electron correlations strongly affect the tunneling rate.

PACS numbers: 73.40.Gk, 03.65.Sq, 73.20.Dx, 73.50.-h

Tunneling plays a fundamental role in many physical phenomena. In the past few decades, much progress has been made in describing it beyond the one-dimensional approximation and understanding how it occurs in many-body systems [1–4]. For charged particles, the tunneling rate can be conveniently controlled by a magnetic field applied transverse to the tunneling direction. Recently this effect was used to probe two-dimensional electron systems (2DES) in semiconductor heterostructures [5–8] and on helium surfaces [9]. However, despite its interest and generality, even the problem of single-electron tunneling decay in a magnetic field remains largely unsolved. Existing results, although often highly nontrivial, are limited to the cases where the potential has either a special form [2,10,11] (e.g., parabolic [10]), or a part of the potential or the magnetic field are in some sense weak [12–16].

Of particular interest for the present paper is tunneling transverse to the field from strongly correlated 2DES [9,17]. In such systems exchange is small, and the tunneling electron can be thought of as moving in the potential created by other electrons. This motion can exponentially strongly affect the tunneling rate. This can be qualitatively understood, because an electron, which tunnels a distance z transverse to the field B and is free to move in the $\mathbf{B} \times \hat{\mathbf{z}}$ direction, has its velocity v_H in this direction incremented by $\omega_c z$ ($\omega_c = eB/m$ is the cyclotron frequency). If initially $v_H = 0$, the energy of motion in the $\hat{\mathbf{z}}$ direction is reduced by $m\omega_c^2 z^2/2$, i.e., there arises a parabolic magnetic barrier for tunneling. On the other hand, if an electron can give the momentum in the $\mathbf{B} \times \hat{\mathbf{z}}$ direction to in-plane excitations in the electron system, v_H can remain small, effectively reducing this barrier. This makes it possible to use tunneling in a magnetic field as a sensitive probe of in-plane electron dynamics in correlated systems.

In this paper we will use an Einstein model in which the in-plane electron motion is a harmonic vibration about an equilibrium position, with one frequency (see Fig. 2 below) [18]. The problem is then effectively reduced to a single-particle problem, which mimics the many-electron one. As we show, the resulting tunneling exponent depends on the dimensionless parameters $\omega_c \tau_0$ and $\omega_0 \tau_0$, where τ_0

is the imaginary time of underbarrier motion for $B = 0$, and ω_0 is a characteristic frequency of in-plane electron vibrations.

For smooth potentials and magnetic fields, the tunneling rate can be found in the WKB approximation, in which the wave function is

$$\psi(\mathbf{r}) = D(\mathbf{r}) \exp[iS(\mathbf{r})] \quad (\hbar = 1). \quad (1)$$

Here, $S(\mathbf{r})$ is the classical action. It is calculated using the classical equations of motion

$$\dot{S} = \mathbf{p} \cdot \dot{\mathbf{r}}, \quad \dot{\mathbf{r}} = \partial H / \partial \mathbf{p}, \quad \dot{\mathbf{p}} = -\partial H / \partial \mathbf{r}, \quad (2)$$

where $H = (\mathbf{p} + e\mathbf{A})^2/2m + U(\mathbf{r})$ is the electron Hamiltonian, and \mathbf{A} is the vector potential of the magnetic field.

In the standard approach to tunneling decay, which applies for $B = 0$ [1,4,19,20], the action S is purely imaginary under the barrier. It is calculated by changing to imaginary time and momentum in Eqs. (2), which then take the form of equations of classical motion in an inverted potential $-U(\mathbf{r})$, with energy $-E \geq -U(\mathbf{r})$. In the presence of a magnetic field, because of broken time-reversal symmetry, the replacement $t \rightarrow -it$, $\mathbf{p} \rightarrow i\mathbf{p}$, $\mathbf{r} \rightarrow \mathbf{r}$, $U(\mathbf{r}) \rightarrow -U(\mathbf{r})$ would lead to a complex Hamiltonian, which makes no sense and indicates that a more general approach is required.

We will find the action S by solving the Hamiltonian Eqs. (2) in complex time and phase space. In contrast to the $B = 0$ case, in the presence of a magnetic field the action is *complex* for *real* \mathbf{r} ; i.e., the decay of the wave function (1) under the barrier is accompanied by spatial oscillations. The tunneling rate is determined by $\text{Im} S$ at the point where the particle emerges from the barrier as a semiclassical wave packet, with real coordinate and real momentum. However, again in contrast to the standard ($B = 0$) analysis, at this point the particle velocity is *finite*, $\text{Re} \dot{\mathbf{r}} \neq 0$.

The trajectories (2) of interest for tunneling decay start for $t = 0$ from the vicinity of the localized metastable state. The initial conditions can be obtained from the known form of the wave function $\psi(\mathbf{r})$ close to the potential well, both in the case where $U(\mathbf{r})$ is parabolic near the minimum and ψ is Gaussian [1,2,4], and where $U(\mathbf{r})$

is nonanalytic in one variable (z), which is of interest for 2DES. In both cases the trajectories (2) are parametrized by two complex parameters $x_{1,2}(0)$, which can be the initial values of the in-plane coordinates $x(0) = x_1(0)$, $y(0) = x_2(0)$ for given $z(0)$, and which in turn determine $\mathbf{p}(0)$ and $S(0)$ [cf. Eq. (7)].

To find the tunneling exponent we note that, once the particle has escaped, it is described by a wave beam which propagates in real time along a *real* classical trajectory $\mathbf{r}_{cl}(t)$. This trajectory can be obtained by analyzing the fan of complex trajectories $\mathbf{r}(t), \mathbf{p}(t)$ (2) for different $x_{1,2}(0)$ and finding such $x_{1,2}(0)$ that, for some t , both $\mathbf{r}(t)$ and $\mathbf{p}(t)$ become *real*,

$$\text{Im } \mathbf{r}(t) = \text{Im } \mathbf{p}(t) = 0. \quad (3)$$

This is a set of equations for complex $x_{1,2}(0)$ and $\text{Im } t$. The number of equations is equal to the number of variables, with account taken of H being real. The $\text{Re } t$ remains undetermined: a change in $\text{Re } t$ in (3) results just in a shift of the particle along the classical trajectory $\mathbf{r}_{cl}(t)$ (see Fig. 1). Such a shift does not change $\text{Im } S$. We note that, in contrast to what happens for $B = 0$, the classical trajectory does *not* have to touch the boundary of the classically forbidden region.

The tunneling exponent \mathcal{R} is given by the value of $\text{Im } S$ at any point on the trajectory \mathbf{r}_{cl} ,

$$\mathcal{R} = 2 \text{Im } S(\mathbf{r}_{cl}). \quad (4)$$

For a physically meaningful solution, $\text{Im } S$ has a parabolic minimum at \mathbf{r}_{cl} as a function of the coordinates transverse to the trajectory, and the outgoing beam is Gaussian near the maximum.

From (3), the tunneling exponent can be obtained by solving the equations of motion (2) in imaginary time, with complex \mathbf{r} . However, such a solution does not give the wave function for real \mathbf{r} between the well and the classical trajectory \mathbf{r}_{cl} . Neither does it tell us where the particle

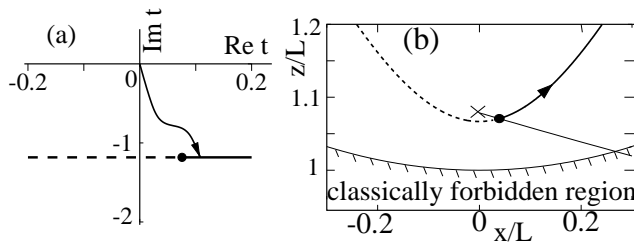


FIG. 1. (a) Complex t plane for integrating the Hamiltonian Eq. (2) in the escape problem. The line $\text{Im } t = \text{const}$ corresponds to the classical trajectory of the outgoing electron. (b) The classical trajectory \mathbf{r}_{cl} on the (x, z) plane. The bold solid lines in (a) and (b) show the “visible” part of the trajectory where the amplitude of the outgoing wave packet exceeds the amplitude of the tail of the underbarrier wave function. The thin solid line in (b) shows where the amplitudes of the two wave functions coincide. It starts from the caustic (\times). The data refer to the potential (8), with $\omega_0\tau_0 = 1.2$ and $\omega_c\tau_0 = 1.2$; time in (a) is in units of τ_0 .

shows up on the classical trajectory. To obtain a complete solution of the tunneling problem, one should take into account the fact that S is a *multivalued* function of \mathbf{r} , even though it is a single-valued function of t and $x_{1,2}(0)$; i.e., several trajectories (2) with different t and $x_{1,2}(0)$ can go through one and the same point \mathbf{r} . The wave function is determined generally by one of the branches of $S(\mathbf{r})$.

Branching and multivaluedness of the action are familiar from the 1D tunneling problem, where $S - S_t \propto (z - z_t)^{3/2}$ near the turning point z_t [19]. In multidimensional systems, branching generally occurs on caustics [21]. In our problem, in contrast to the usually considered case, the trajectories $\mathbf{r}(t)$ will be *complex*, as will also be the caustics. Caustics of most general type are *envelopes* of the trajectories $\mathbf{r}(t)$ (2). They are given by the equation

$$J(\mathbf{r}) = 0, \quad J(\mathbf{r}) = \frac{\partial(x, y, z)}{\partial[x_1(0), x_2(0), t]}. \quad (5)$$

The prefactor in the WKB wave function (1) is $D = \text{const} \times J^{-1/2}$. Therefore the WKB approximation does not apply close to the caustic (cf. [21]).

The caustic of interest is the one where the analytically continued wave functions of the outgoing semiclassical wave and the WKB tail of the intrawell state are connected. The amplitude of the semiclassical wave incident on the barrier from $z \rightarrow \infty$ should be set equal to zero. Local analysis near the caustic is similar to that in the 1D case. It is convenient to change to the variables x' , y' , and z' which are locally parallel and perpendicular to the caustic surface, respectively. We set $z' = 0$ on the caustic. For small $|z'|$,

$$S(x', y', z') \approx S(x', y', 0) + a_1 z' + a_2 z'^{3/2} \quad (6)$$

[the coefficients $a_{1,2} \equiv a_{1,2}(x', y')$ can be expressed in terms of the derivatives of S, \mathbf{r} over $x_{1,2}(0), t$ on the caustic]. As in the 1D problem, the prefactor in (1) depends on the distance to the caustic as $D \propto (z')^{-1/4}$. However, in the present case S contains a linear term $a_1 z'$, and therefore the momentum perpendicular to the caustic is *finite*. We note that Eq. (5) and the condition $\text{Im } \mathbf{r} = 0$ define a line in real space, which can be called a caustic line.

For real \mathbf{r} , there is a *switching surface* which separates the ranges where $\text{Im } S(\mathbf{r})$ is smaller for one or the other of the solutions connected on the caustic [22]. Only the solution with the smaller $\text{Im } S$ should be held in the WKB approximation. It is this condition that determines *where* the outgoing wave shows up from beneath the tail of the intrawell state. The switching surface starts from the caustic line, where the branches of S merge together. The cross sections of the switching surface and the caustic line by the plane (x, z) are shown in Fig. 1.

We now apply these general results to a simple model which is relevant to electrons on helium. The corresponding geometry is shown in Fig. 2a. For typical densities $n \sim 10^8 \text{ cm}^{-2}$ and temperatures $T \lesssim 1 \text{ K}$, these electrons form a Wigner crystal [23] or a nondegenerate liquid [24].

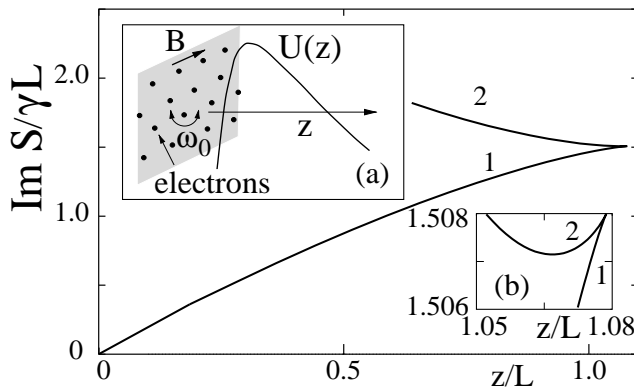


FIG. 2. Two branches of the action on the symmetry axis $x = 0$ as a function of the tunneling coordinate z before the branching point, for the same parameters as in Fig. 1. The vicinity of the cusp at z_c is zoomed in inset (b). Inset (a): The geometry of tunneling from a correlated 2DES transverse to a magnetic field; ω_0 is the Einstein vibration frequency in the Wigner solid.

In both these cases, the characteristic frequency of vibrations about a (quasi)equilibrium in-plane position is $\omega_0 = (2\pi e^2 n^{3/2}/m)^{1/2}$.

The initial conditions for the equations of underbarrier motion (2) can be chosen at an arbitrary plane $z = \text{const}$ close to the electron layer and yet deep enough under the barrier so that the electron wave function is semiclassical. We set $z \equiv z(0) = 0$ on this plane. In the Einstein model, the potential for in-plane motion for $z = 0$ is $(m\omega_0^2/2)(x^2 + y^2)$, and $\psi(x, y, z = 0)$ is Gaussian in x, y . Then for $t = 0$ in (2),

$$\begin{aligned} z(0) &= 0, & p_z(0) &= i\gamma, \\ S(0) &= \frac{im\omega_0}{2} [x^2(0) + y^2(0)], \end{aligned} \quad (7)$$

where $\gamma = [2mU(\mathbf{r} = \mathbf{0})]^{1/2}$ is the reciprocal localization length in the z direction, $\gamma \gg (m\omega_0)^{1/2}$ (the energy of the localized state is set equal to zero). The initial values of the in-plane momentum components $p_j(0) = \partial S(0)/\partial x_j(0) = im\omega_0 x_j(0)$ (where $j = 1, 2$ enumerates the in-plane coordinates).

For electrons on helium, tunneling occurs if there is applied an electric field E_\perp which pulls electrons away from the helium surface [25]. The tunneling barrier is formed by the image potential and the potential of this field. It is nearly triangular at distances from the surface which are much greater than the effective Bohr radius γ^{-1} . The barrier width $L = \gamma^2/2meE_\perp$ for $B = 0$. Typically $L \ll n^{-1/2}$, and therefore the effective electron potential energy is well represented by

$$U(\mathbf{r}) = \frac{m\omega_0^2}{2} (x^2 + y^2) + \frac{\gamma^2}{2m} \left(1 - \frac{z}{L}\right) \quad (z > 0). \quad (8)$$

With (8), the equations of motion (2) become linear and can be readily solved. The symmetry of the potential

$U(x, y, z) = U(\pm x, \pm y, z)$ gives rise to a specific symmetry of the set of the trajectories (2), and one can show that the caustic of interest intersects the real space for $x = 0$ and some $z = z_c$ ($z_c = L$ for $B = 0$).

For \mathbf{B} along the y axis (see Fig. 2a), the motion in the y direction is decoupled and the problem becomes two dimensional. For $z \leq z_c$, the function $\text{Im} S$ has two branches, each of which is symmetrical in x . The branch 1 describes the tail of the intrawell wave function before branching. It has a minimum at $x = 0$ for given z , and monotonically increases with $|x|$ and z . As expected, the slope $\partial \text{Im} S/\partial z$ is finite at the branching point z_c . The branch 2 corresponds to the wave “reflected” from the caustic. This branch is nonmonotonic in z for $x = 0$, with a minimum at $z_m < z_c$. For $z_m < z \leq z_c$, it has two symmetrical *minima* for $x \neq 0$. They lie on the classical trajectory shown in Fig. 1b, and merge together for $z = z_m$.

As discussed above, $\text{Im} S$ is constant on the classical trajectory in Fig. 1b. This trajectory goes through the point $x = 0, z = z_m$ and is symmetrical in x . Although the potential $U(\mathbf{r})$ is even in x and is minimal for $x = 0$, the escaped particle “shows up” on the classical trajectory for finite x . This happens where $\text{Im} S_1(\mathbf{r}_{\text{cl}}) = \text{Im} S_2(\mathbf{r}_{\text{cl}}) = \mathcal{R}/2$ (the subscript enumerates the branches in Fig. 2). The particle has finite velocity and moves away from the barrier.

Since the point $x = 0, z = z_m$ lies on the classical trajectory of interest (although on the section “hidden” by the tail of the intrawell state), the tunneling exponent is given by $\mathcal{R} = 2 \text{Im} S_2(x = y = 0, z_m)$ and can be calculated in imaginary time, with imaginary $x(0)$:

$$\begin{aligned} \tilde{\mathcal{R}} &= -\nu_0^2 \tau^3 - 3\nu_0(1 - \tau)^2 + 3(1 + \nu_0)(1 - \tau) \\ &\quad + 3\nu^2 \tau, \quad \mathcal{R} = 2\gamma L \tilde{\mathcal{R}}/3\nu^2, \end{aligned} \quad (9)$$

where $\nu_0 = \omega_0 \tau_0, \nu_c = \omega_c \tau_0$ are the dimensionless in-plane and cyclotron frequencies ($\tau_0 = 2mL/\gamma$ is the “duration” of underbarrier motion in imaginary time for $B = 0$), $\nu^2 = \nu_0^2 + \nu_c^2$, and $\tau = it/\tau_0$ is given by the equation

$$[\nu^2 \nu_0(1 - \tau) - \nu_c^2] \tanh \nu \tau = \nu(\nu_0^2 \tau - \nu^2). \quad (10)$$

The tunneling exponent as a function of ω_0, ω_c is shown in Fig. 3. For $\omega_0 = 0$ (no electron-electron interaction), the magnetic barrier makes tunneling impossible for $\omega_c \tau_0 \geq 1$ [9] (see curve 1; $\tau \rightarrow \infty$ for $\nu_0 = 0, \nu_c \rightarrow 1$). Even comparatively weak in-plane confinement eliminates this effect. The reduction of the tunneling suppression is significant already for small $\omega_0 \tau_0$, and increases fast with increasing $\omega_0 \tau_0$.

The above results provide an explanation of the magnetic field dependence of the tunneling exponent for electrons on helium, which was observed to be *much weaker* [9] than would be expected from the single-electron theory. Detailed comparison with the data [9] will be discussed elsewhere [18], where the model will

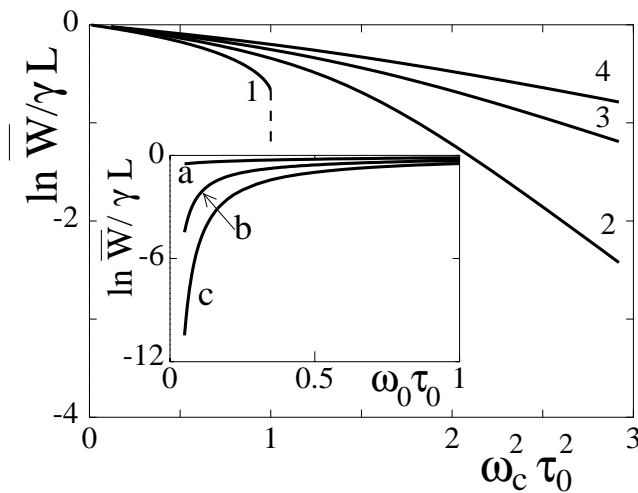


FIG. 3. The dependence of the tunneling rate on magnetic field, $\bar{W} = W(B)/W(0)$. The curves 1 to 4 refer to $\omega_0\tau_0 = 0, 0.2, 0.4, 0.6$. Magnetic field eliminates single-electron tunneling for $\omega_c\tau_0 \geq 1$ (cf. curve 1). Inset: tunneling exponent vs in-plane frequency ω_0 for $\omega_c^2\tau_0^2 = 1.0, 2.0, 3.0$ (curves *a, b, c*).

also be extended in order to include the realistic vibrational spectrum of the Wigner solid. At zero temperature this extension does not change the results significantly, because electron tunneling is accompanied by excitation of mostly short-wavelength vibrations, which are reasonably well described by the Einstein model used above.

In conclusion, we have shown that, under suitable conditions ($\omega_c\tau_0 \geq 1, \omega_0\tau_0 \geq 1$), correlations in a 2DES can very strongly affect the rate of tunneling escape transverse to a magnetic field. We have also shown that the problem of single particle tunneling in a magnetic field can be solved in the semiclassical limit by analyzing the Hamiltonian trajectories of the particle in complex space and time. The connection of decaying and propagating waves occurs on caustics of the set of these trajectories. This approach does not require us to consider any piece of the electron potential or the magnetic field as a perturbation. It gives us an escape rate which is generally *exponentially* smaller than the probability for a particle to reach the boundary of the classically accessible range $U(\mathbf{r}) = E$. Finally, we have obtained explicit results for a simple model of an electron tunneling from a helium surface transverse to a magnetic field.

We are grateful to V.N. Smelyanskiy who participated in this work at the early stage, and to D. Farber for help with numerical calculations. This research was supported in part by the NSF through Grant No. PHY-9722057.

- [1] J. S. Langer, *Ann. Phys. (N.Y.)* **41**, 108 (1967); S. Coleman, *Phys. Rev. D* **15**, 2929 (1977).
- [2] A. O. Caldeira and A. J. Leggett, *Ann. Phys. (N.Y.)* **149**, 374 (1983).
- [3] *Quantum Tunneling in Condensed Matter*, edited by Yu. Kagan and A. J. Leggett (Elsevier, New York, 1992).
- [4] A. Auerbach and S. Kivelson, *Nucl. Phys.* **B257**, 799 (1985).
- [5] J. Smoliner *et al.*, *Phys. Rev. Lett.* **63**, 2116 (1989); G. Rainer *et al.*, *Phys. Rev. B* **51**, 17 642 (1995).
- [6] J. P. Eisenstein *et al.*, *Phys. Rev. B* **44**, 6511 (1991); S. Q. Murphy *et al.*, *Phys. Rev. B* **52**, 14 825 (1995).
- [7] L. Zheng and A. H. MacDonald, *Phys. Rev. B* **47**, 10 619 (1993).
- [8] T. Ihn *et al.*, *Phys. Rev. B* **54**, R2315 (1996); M. J. Yang *et al.*, *Phys. Rev. Lett.* **78**, 4613 (1997); M. Lakrimi *et al.*, *Phys. Rev. Lett.* **79**, 3034 (1997).
- [9] L. Menna, S. Yücel, and E. Y. Andrei, *Phys. Rev. Lett.* **70**, 2154 (1993).
- [10] H. A. Fertig and B. I. Halperin, *Phys. Rev. B* **36**, 7969 (1987).
- [11] P. Ao, *Phys. Rev. Lett.* **72**, 1898 (1994); *Phys. Scr.* **T69**, 7 (1997).
- [12] B. I. Shklovskii, *JETP Lett.* **36**, 51 (1982); B. I. Shklovskii and A. L. Efros, *Sov. Phys. JETP* **57**, 470 (1983).
- [13] Qin Li and D. J. Thouless, *Phys. Rev. B* **40**, 9738 (1989).
- [14] T. Martin and S. Feng, *Phys. Rev. B* **44**, 9084 (1991).
- [15] J. Haidu, M. E. Raikh, and T. V. Shahbazyan, *Phys. Rev. B* **50**, 17 625 (1994).
- [16] B. Hellfer and J. Sjöstrand, *Ann. Scuola Norm. Sup. Pisa Cl. Sci.* **14**, 625 (1988).
- [17] Jongsoo Yoon *et al.*, *Phys. Rev. Lett.* **82**, 1744 (1999); A. P. Mills, Jr. *et al.*, *Phys. Rev. Lett.* **83**, 2805 (1999), and references therein.
- [18] T. Sharpee *et al.* (to be published).
- [19] L. D. Landau and E. M. Lifshitz, *Quantum Mechanics: Non-relativistic Theory* (Pergamon, New York, 1977); M. V. Berry and K. E. Mount, *Rep. Prog. Phys.* **35**, 315 (1972).
- [20] U. Eckern and A. Schmid, in Ref. [3], p. 145.
- [21] M. V. Berry, *Adv. Phys.* **25**, 1 (1976); L. S. Schulman, *Techniques and Applications of Path Integration* (Wiley, New York, 1981).
- [22] For classical systems, the occurrence of switching lines on the tails of distribution was discussed by M. I. Dykman, M. M. Millonas, and V. N. Smelyanskiy, *Phys. Lett. A* **195**, 53 (1994).
- [23] C. C. Grimes and G. Adams, *Phys. Rev. Lett.* **42**, 795 (1979); D. S. Fisher, B. I. Halperin, and P. M. Platzman, *Phys. Rev. Lett.* **42**, 798 (1979).
- [24] M. I. Dykman *et al.*, *Phys. Rev. Lett.* **70**, 3975 (1993); M. J. Lea and M. I. Dykman, *Physica (Amsterdam)* **251B**, 628 (1998).
- [25] M. Ya. Azbel and P. M. Platzman, *Phys. Rev. Lett.* **65**, 1376 (1990).